1alpha,25-Dihydroxyvitamin D(3) triggered vitamin D receptor and farnesoid X receptor-like effects in rat intestine and liver in vivo.

ARTICLE *in* BIOPHARMACEUTICS & DRUG DISPOSITION · NOVEMBER 2009

Impact Factor: 2.34 · DOI: 10.1002/bdd.682 · Source: PubMed

BIOPHARMACEUTICS & DRUG DISPOSITION
Biopharm. Drug Dispos. **30**: 457–475 (2009)
Published online 13 September 2009 in Wiley InterScience
(www.interscience.wiley.com) **DOI**: 10.1002/bdd.682

1α,25-Dihydroxyvitamin D_3 Triggered Vitamin D Receptor and Farnesoid X Receptor-like Effects in Rat Intestine and Liver *In Vivo*

Edwin C. Y. Chow[a], Han-Joo Maeng[a], Shanjun Liu[a], Ansar A. Khan[b], Geny M. M. Groothuis[b], and K. Sandy Pang[a,*]

[a]*Department of Pharmaceutical Sciences, Leslie Dan Faculty of Pharmacy, University of Toronto, Canada*
[b]*Pharmacokinetics, Toxicology and Targeting, Department of Pharmacy, University of Groningen, The Netherlands*

ABSTRACT: 1α,25-Dihydroxyvitamin D_3 ($1,25(OH)_2D_3$), a natural ligand of the vitamin D receptor (VDR), was found to increase the rat ileal Asbt and bile acid absorption. The effects of VDR, whose expression is low in liver, on hepatic transporters and enzymes are unknown. Protein and mRNA levels of target genes in the small intestine, colon and liver after intraperitoneal dosing of $1,25(OH)_2D_3$ (0–2.56 nmol/kg/day for 4 days) to the rat were determined by Western blotting and qPCR, respectively. The $1,25(OH)_2D_3$ treatment increased total Cyp3a protein and Cyp3a1 mRNA expressions in the proximal small intestine, and the short heterodimer partner (SHP), the fibroblast growth factor 15 (FGF15), organic solute transporter (Ostα and Ostβ) mRNA and Asbt protein expressions in the ileum. About 50% higher portal bile acid concentration (65.1 ± 14.9 vs 41.9 ± 7.8 μM, $p < 0.05$) and elevated expressions of the hepatic farnesoid X receptor (FXR) and SHP mRNA resulted with $1,25(OH)_2D_3$ treatment. Increased Bsep and Ostα mRNA expressions in liver and a >50% reduction in the Cyp7a1 protein level ($p < 0.05$) and cholesterol metabolism in rat liver microsomes ($p = 0.002$), likely consequences of the bile acid-FXR-SHP cascade and activation of the signaling pathway for Cyp7a1 inhibition by FGF15, were found. Increased hepatic multidrug resistance-associated protein (Mrp3) and multidrug resistance protein 1a (Mdr1a) mRNA and P-gp protein were also observed. It was concluded that the changes in hepatic transporters and enzymes in the rat were indirect, secondary effects of the liver FXR-SHP cascade due to increased intestinal absorption of bile acids and elevated levels of FGF15, events that led to the activation of FXR. Copyright © 2009 John Wiley & Sons, Ltd.

Key words: 1α,25-dihydroxyvitamin D_3; nuclear receptors or NRs; the vitamin D receptor or VDR; farnesoid X receptor or FXR; short heterodimer partner or SHP; fibroblast growth factor 15 or FGF15; Western blotting; qRT-PCR; liver; intestine; transporters; enzymes; bile acids; Cyp3a; Cyp7a1; Asbt; Bsep; P-gp; Mrp2; Mrp3; Mrp4

Introduction

Nuclear receptors (NRs) play an important role in the regulation of hepatobiliary transporters and enzymes in bile acid homeostasis [1]. The farnesoid X receptor (FXR; NR1H4) is the most important bile acid sensor and responds to high bile acid concentrations by inducing the short heterodimer partner (SHP; NR0B2) [2], which, in turn inhibits the liver receptor homolog 1 (LRH-1). One of the major FXR effects is the down-regulation of cholesterol 7α-hydroxylase, CYP7A1 [2], the rate-limiting enzyme for the

*Correspondence to: Faculty of Pharmacy, University of Toronto, 144 College Street, Toronto, Ontario, Canada M5S 3M2. E-mail: ks.pang@utoronto.ca

Received 8 April 2009
Revised 13 July 2009
Accepted 7 August 2009

formation of bile acids from cholesterol in the liver [3]. In contrast, the rodent liver X receptor-α (LXRα; NR1H3), liver receptor homolog-1 (LRH-1; NR5A2) and hepatocyte nuclear factor 4α (HNF-4α; NR2A1) are known to increase CYP7A1 [2,4,5]. The activation of FXR in the intestine increases the fibroblast growth factor 15 (FGF15) or its complement, FGF19, in man [6], a hormone that binds to the fibroblast growth factor receptor 4 (FGFR4) of the liver to decrease CYP7A1 [6,7]. The mechanism involves the mitogen-activated protein kinase/extracellular signal-regulated kinase 1/2 (MAPK/Erk1/2) pathway that mediates FGF19 inhibition of CYP7A1 without involving SHP; in humans, bile acid-activated FXR is able to induce FGF19 in hepatocytes to inhibit CYP7A1 by an autocrine/paracrine mechanism [6]. FXR further counteracts the hepatic cytotoxicity of bile acids by decreasing the expression of sodium taurocholate co-transporting polypeptide (NTCP; SLC10A1) at the sinusoidal membrane to reduce bile acid uptake [8] and inducing the canalicular transporters, the bile salt export pump (BSEP; ABCB11) [2] and the multidrug resistance associated protein 2 (MRP2; ABCC2) [9] for the excretion of bile acids and bile salts. Transcription factors are also affected by FXR: the hepatocyte nuclear factor 1-alpha (HNF-1α), which is highly regulated by HNF-4α, activates the rat Ntcp and the organic anion transporting polypeptides, Oatp1a1 (Slco1a1) and Oatp1a4 (Slco1a4) [10], transporters that promote bile acid uptake into the rat liver; inhibition of HNF-1α or HNF-4α would also lead to decreased Ntcp and bile acid uptake.

In the rat intestine, bile acids are reabsorbed into enterocytes through the apical sodium dependent bile acid transporter (Asbt; SLC10A2) [1]. Increased bile acids in enterocytes trigger the activation of FXR. FXR increases SHP, organic solute transporter (Ostα and Ost*β*), and FGF15 to promote bile acid efflux and signals the down-regulation of Cyp7a1 in the rat liver [2,7,11]. Due to the absence of LRH-1 in rodent ileum, the negative feedback mechanism of the FXR to down-regulate rat Asbt to decrease bile acid absorption is lacking [12]. Despite these species differences, FXR remains as an important nuclear receptor that is involved in the regulation of bile acid reabsorption in the intestine and bile acid synthesis in the liver.

The vitamin D receptor (VDR; NR1I1), a member of the steroid/thyroid hormone NR superfamily, which exhibits significant homology with the xenobiotic NRs, the pregnane X receptor (PXR; NR1I2) and the constitutive androstane receptor (CAR; NR1I3), is important in the regulation of transporters and enzymes in bile acid homeostasis [13]. Like PXR and CAR, activation of VDR induces human CYP3A4 [14,15] and rat Cyp3a9 [16] and Cyp3a1 [15,17]. 1α,25-Dihydroxyvitamin D_3 [1,25$(OH)_2D_3$], the active form of vitamin D, is the natural ligand of VDR, whereas lithocholic acid, a toxic bile acid and another ligand of VDR, was found to induce Cyp3a in the murine liver and intestine [18] and in intestinal slices of the rat and human [15], serving as a detoxification mechanism pathway of bile acids in the colon. In addition, 1,25$(OH)_2D_3$ was implicated to induce the Asbt and increase bile acid absorption [19] as well as rat multidrug resistance-associated proteins Mrp2, Mrp3 and Mrp4 [20] of the small intestine via the VDR in the rat. 1,25$(OH)_2D_3$ increased the expression of murine Mrp3 (Abcc3) in the colon [21], hydroxysteroid sulfotransferase (SULT2A1) in VDR-transfected cells [22], and MRP2 and MRP4 (ABCC4) protein and MDR1 mRNA and protein in Caco-2 cells [23]. A vitamin D response element was further identified for MDR1 [24].

To date, there exists little or no systematic study that describes the effects of 1,25$(OH)_2D_3$-liganded VDR nor on the regulation of transporters and enzymes of bile acid homeostasis *in vivo*. Ogura *et al*. [25] recently reported on changes in hepatic and renal mRNA expression of transporters and enzymes in mice that underwent sham or bile duct ligation and were treated with an extremely high dose (31 nmol/kg) of 1α-hydroxyvitamin D_3, an inert precursor of 1,25$(OH)_2D_3$. However, the physiology of the animal was compromised by bile duct ligation and the protein expression and function of the transporters and enzymes was not evaluated. Moreover, 1α-hydroxyvitamin D_3 may not be an effective modulator of intestinal-related effects since the prodrug requires activation by the 25-hydroxylase in the liver to form the active compound, 1,25$(OH)_2D_3$ [26].

The objective of this study was to examine the role of VDR on transporters and enzymes in

DOI: 10.1002/bdd

the intestine and liver of the rat *in vivo*. Relatively high levels of VDR exist in the rat intestine, where VDR-related changes have been observed [14,15,19,23]. In comparison, very low levels of VDR exist in rat hepatocytes [27], and little or no VDR-related changes in transporter and enzyme genes are expected to occur in the liver. Previous *in vitro* studies with precision cut rat liver slices confirmed this notion, and failed to show observable induction of Cyp3a1, Cyp3a2, or Cyp3a9 by $1,25(OH)_2D_3$ [15]. However, increased portal bile acid absorption as a result of elevated Asbt in the rat *in vivo* by $1,25(OH)_2D_3$ treatment [12] could trigger indirect or secondary changes in hepatic transporters and enzymes due to the activation or inhibition of other nuclear receptors, especially, FXR. Hence, we wished to identify the direct, inductive VDR effects on intestinal Asbt and Cyp and both the direct and indirect effects on the liver by studying the changes in protein and mRNA levels of VDR and FXR target genes in the intestine and liver after $1,25(OH)_2D_3$ treatment in the rat *in vivo*. The hypothesis that changes in the liver *in vivo* were secondary, FXR-related effects and not VDR effects was tested. The study further examined the possible VDR effects on other NRs in the rat liver, since an antagonism of the VDR on chenodeoxycholate-activated FXR effect had been documented in FXR- and VDR-transfected HepG2 cells [28].

Methods

Materials

$1,25(OH)_2D_3$ powder was purchased from Sigma-Aldrich Canada (Mississauga, ON, Canada). Antibodies to villin (C-19) and rat Cyp7a1 (N-17) were purchased from Santa Cruz Biotechnology (Santa Cruz, CA); anti-Mrp2 (ALX-801-016-C250), from Alexis Biochemicals, San Diego, CA; anti-P-gp (C219), from Abcam, Cambridge, MA; anti-Gapdh (14C10), from Cell Signaling Technology, Danvers, MA; anti-VDR (MA1-710) was purchased from Affinity BioReagents, Golden, CO; anti-Cyp3a2 antibodies (458223) that failed to distinguish from Cyp3a1 or Cyp3a9 were purchased from BD Biosciences, Mississauga, ON. Other antibodies were kind gifts from various investigators: anti-Oatp1a1, anti-Oatp1a4, and anti-Ntcp (Dr Allan W. Wolkoff, Albert Einstein College of Medicine, the Bronx, NY), anti-Oatp1b2 (Dr Richard B. Kim, University of Western Ontario, ON); anti-Asbt (Dr Paul A. Dawson, Wake Forest University, Salem, NC); anti-Mrp3 (Dr Yuichi Sugiyama, University of Tokyo, Japan); anti-Mrp4 (Dr John D. Schuetz, St Jude Children's Research Hospital, TN); anti-Bsep (Dr Bruno Stieger, University Hospital, Zurich, Switzerland). All other reagents were purchased from Sigma-Aldrich Canada (Mississauga, ON, Canada) and Fisher Scientific (Mississauga, ON, Canada).

$1,25(OH)_2D_3$ and vehicle (corn oil) treatment in rats in vivo

$1,25(OH)_2D_3$ was dissolved in anhydrous ethanol, and the concentration was measured spectrophotometrically at 265 nm (UV-1700, Shimadzu Scientific Instruments, MD); then the solution was diluted in filtered sterile corn oil (Sigma-Aldrich, ON) for injection. Male Sprague-Dawley rats (260–280 g), purchased from Charles River (St Constant, QC), were given water and food *ad libitum* and maintained under a 12:12-h light and dark cycle in accordance with animal protocols approved by the University of Toronto (ON, Canada). Rats ($n = 4$ in each group) were injected with 0, 0.64, 1.28 and 2.56 nmol/kg/day $1,25(OH)_2D_3$ in 1 ml/kg corn oil intraperitoneally for 4 days. At 24 h following the last day of $1,25(OH)_2D_3$ treatment, the rats were anesthetized with ketamine and xylazine (90 mg/kg and 10 mg/kg, respectively) by intraperitoneal injection. An aliquot (0.5 ml) of portal and systemic blood was collected and centrifuged at 3000 rpm for 10 min to obtain serum.

Blood analysis and preparation of tissues

The portal bile acid concentration was determined using a total bile acids assay kit (BQ042A-EALD from BioQuant, San Diego, CA) following the manufacturer's protocol. Serum alanine aminotransferase was assayed with a reagent

DOI: 10.1002/bdd

kit (BQ004A-CR) following the manufacturer's protocol.

After blood collection, the portal vein was cannulated and flushed with 50 ml of ice-cold physiological saline solution. The small intestine was removed and placed on ice, and cut into eight segments [19]. Segment 1 (S1) is the duodenum, spanning from the pyloric ring to the ligament of Treitz; segment 2 (S2) is the proximal jejunum segment of equal length that is immediately distal to the ligament of Treitz. The remaining small intestine was then divided into six segments of equal length (S3 to S8, with S8 representing the ileum proximal to the ileocecal junction) [19]. Only the S1, S2, S7 and S8 segments were used in this study. Enterocytes were isolated by mucosal scraping of everted tissue with a tissue-scraper [29] ($n = 4$). The colon (taken as a 10 cm section after the ileocecal junction) was removed of fecal matters via flushing with 1 mM phenylmethylsulfonyl fluoride (PMSF) in 0.9% NaCl solution, and stored in the same solution. Enterocytes from the colon were removed by mucosal scraping. Enterocytes from all segments were immediately snap frozen in liquid nitrogen and stored at −80°C until analyses. The liver was removed, weighed, cut to small pieces, and snap frozen in liquid nitrogen, then stored in a −80°C freezer for future analyses.

Preparation of subcellular fractions from enterocytes. Frozen mucosal scrapings (50–100 mg of tissue) from intestinal segments and the colon were immediately mixed with 1 ml of Trizma HCl (0.1 M, pH 7.4) buffer containing 1% protease inhibitor cocktail (Sigma-Aldrich, ON) and homogenized on ice for three 30 s periods at 8000 rpm using an Ultra-turrax T25 homogenizer (Janke & Kunkel, Staufen, Germany), then sonicated for 10 s. The samples were centrifuged at $1000 \times g$ at 4°C for 10 min while the pellet, the crude nuclear protein fraction, was resuspended in nuclear buffer (60 mM KCl, 15 mM NaCl, 5 mM $MgCl_2 \cdot 6H_2O$, 0.1 mM EGTA, 300 mM sucrose, 0.5 mM dithiothreitol (DTT), 0.1 mM PMSF, 300 mM sucrose, 15 mM Trizma HCl pH 7.4) containing 1% protease inhibitor cocktail. The nuclear fraction was used for the Western blot analysis of VDR expression. The supernatant was transferred to a new tube and spun again at $21000 \times g$ at 4°C for 1 h to yield another supernatant (crude cytosolic fraction) and pellet (crude membrane fraction); the pellet was resuspended in the same homogenizing buffer and used for Western blot analyses of the intestinal transporters.

Preparation of subcellular fractions of liver tissue. For the preparation of the crude membrane fraction, ~0.5 g of weighed liver tissue was homogenized in the crude membrane homogenizing buffer (250 mM sucrose, 10 mM HEPES and 10 mM Trizma base, pH 7.4) containing 1% protease inhibitor cocktail as described above. The resultant homogenate was centrifuged at $9000 \times g$ for 10 min at 4°C. The supernatant was transferred to an ultracentrifuge tube and spun at $33000 \times g$ for 60 min at 4°C. The resultant pellet yielded the crude membrane protein fraction, and was placed in resuspension buffer (50 mM mannitol, 20 mM HEPES, 20 mM Trizma base, pH 7.4) containing 1% protease inhibitor cocktail, and was used for Western blot analyses of hepatic transporters.

For the preparation of the microsomal fraction, ~0.5 g of liver tissue was homogenized with the microsome homogenizing buffer (250 mM sucrose, 10 mM Trizma HCl, 1 mM EDTA, pH 7.4) containing 1% protease inhibitor cocktail as described above. The homogenate was centrifuged at $9000 \times g$ for 10 min at 4°C. The supernatant was transferred to an ultracentrifuge tube and spun at $100000 \times g$ for 60 min at 4°C. The resulting pellet containing the microsomes was resuspended in the same homogenizing buffer and used for Western blot analyses of cytochrome P450 enzymes.

Protein concentration of the samples was assayed by Lowry method using bovine serum albumin as the standard [30]. Samples were then stored at −80°C until Western blot analyses.

Liver microsomal Cyp7a1 activity

Liver tissue was homogenized with a Potter-Elvehjem homogenizer in the microsome homogenizing buffer described above in the absence of protease inhibitors, since we wished to test for the functional activity of Cyp7a1. The microsomal

DOI: 10.1002/bdd

fraction, obtained by differential centrifugation as described above, was used to examine Cyp7a1 activity outlined by Hylemon *et al*. [31]. Microsomal protein (50 µl of 40 mg/ml solution) in microsomal reaction buffer [415 µl containing 100 mM potassium phosphate, 50 mM NaF, 1 mM EDTA, 0.015% 3-[(3-cholamidopropyl)dimethylammonio]-1-propanesulfonate (CHAPS), 20% glycerol and 5 mM DTT] was pre-incubated for 5 min at 37°C. The reaction was initiated by the addition of a nicotinamide adenine dinucleotide phosphate (NADPH) generating system (25 µl of solution A and 5 µl of solution B, BD Biosciences) and 5 µl of 10 mM cholesterol in acetone, resulting in 2 mg of microsomal protein in 500 µl of incubation mixture. After 30 min of incubation, the reaction was terminated by the addition of 15 µl of ice-cold 20% sodium cholate and then 15 µl of the internal standard, 92 µg/ml 7β-hydroxycholesterol (Steraloids Inc, Newport, RI), was added. The 7α-hydroxycholesterol formed in the reaction was converted into 7α-hydroxy-4-cholesten-3-one upon incubation with 44 µl 12.5 U/ml cholesterol oxidase (Sigma) in cholesterol oxidase buffer (10 mM potassium phosphate, 20% glycerol and 1 mM DTT) for 10 min at 37°C. This reaction was terminated by the addition of 1 ml of ice-cold methanol. The product, 7α-hydroxy-4-cholesten-3-one, was extracted into 9 ml of hexane after mixing the contents vigorously for 15 min, followed by centrifugation at 4°C for 5 min at $5000 \times g$. After evaporation of the hexane extract under N_2 (Linde Canada, Ltd, Mississauga, ON), the residue was reconstituted in 100 µl mobile phase (acetonitrile:methanol 70:30 v/v), and 20 µl was injected into the Shimadzu HPLC (LC 10AT pump, SPD-10A UV-Vis detector, SIL-10A autoinjector and SCL-10A system controller). Separation was achieved with an Altex 10 µm C-18 reverse phase column (4.6 mm × 250 mm) at flow rates varying from 0.7 to 2 ml/min, with detection carried out at 240 nm; data integration was performed by the software, Star Chrom Lite®. Standards (0.05 to 2.5 nmole) containing varying amounts of 7α-hydroxycholesterol (Steraloids Inc.) were processed under identical conditions and were converted into 7α-hydroxy-4-cholesten-3-one for construction of the calibration curve. The plot of the peak area ratios of 7α-hydroxy-4-cholesten-3-one/internal standard against 7α-hydroxycholesterol concentration was linear. The reaction rate was normalized to the amount of microsomal protein.

Western blotting

Samples (20 or 50 µg total protein) were mixed with the loading buffer containing 0.1 M of DTT and incubated at an optimized, denaturing condition (room temperature for 30 min, 37°C for 15 min or 95°C for 2 min). Loaded proteins ($n = 3$ or 4 for each treatment group) were separated by 7.5% or 10% SDS-polyacrylamide gels that were overlaid with a 4% polyacrylamide stacking gel at 100 V. After separation, the proteins were transferred onto a nitrocellulose membrane (Amersham Biosciences, Piscataway, NJ). The membrane was blocked with 5% (w/v) skim milk in Tris-buffered saline (pH 7.4) and 0.1% Tween 20 (TBS-T) (Sigma-Aldrich, ON) for 1 h at room temperature, and then washed with 0.1% TBS-T for 10 min. The membrane was incubated with primary antibody solution (1:1000 to 1:5000 in 2% skim milk in 0.1% TBS-T) overnight at 4°C. On the next morning, the membrane was washed with 0.1% TBS-T three times for 10 min each before incubation with the secondary antibody (1:2000; anti-rat for VDR; 1:2000; anti-rabbit for Mrp3, Mrp4, Bsep, Oatp1a1, Oatp1a4, Oatp1b2, Ntcp, Asbt, rat glyceraldehyde-3-phosphate dehydrogenase (Gapdh) and Cyp3a2; anti-goat for villin and Cyp7a1; anti-mouse for P-gp and Mrp2) with 2% skim milk in 0.1% TBS-T for 2 h at room temperature, and again washed three times with 0.1% TBS-T for 10 min each. The bands were visualized using chemiluminescence reagents (Amersham Biosciences, Piscataway, NJ) and quantified by scanning densitometry (NIH Image software; http://rsb.info.nih.gov/nih-image/). The band intensity of the target protein was normalized against that for villin for intestinal samples or Gapdh for intestinal VDR and liver samples, to correct for the loading errors.

Quantitative real-time polymerase chain reaction (qRT-PCR or real-time PCR)

Total RNA was obtained from 50–100 mg of scraped enterocytes and liver tissue using the

DOI: 10.1002/bdd

TRIzol extraction method (Sigma-Aldrich) according to the manufacturer's protocol, with modifications. The extracted RNA pellet was then air dried and dissolved in TE buffer (Applied Biosystems Canada, ON). Total RNA was quantified by UV spectrometry measured at 260 nm. The purity was checked by ratios of the readings at 260/280 nm and 260/230 nm ($\geqslant$1.8). cDNA was immediately synthesized from RNA samples, using a high capacity cDNA reverse transcription kit (Applied Biosystems Canada, ON) and following the instructions provided by the manufacturer. In brief, 1.5 μg of total RNA was transcribed in a 20 μl reaction volume on the Applied Biosystems 2720 Thermal Cycler. The program consisted of 10 min for annealing at 25°C, 120 min for reverse transcription at 37°C, and 5 min for inactivation at 85°C. A real-time quantitative polymerase chain reaction (qRT PCR) was performed with two detection systems (SYBR Green or Taqman assay), depending on the availability of primer sets. Information on primer sequences is summarized in Table 1. These primer sets were analyzed using BLASTn to ensure primer specificity for the gene of interest (http://www.ncbi.nlm.nih.gov/BLAST/). A PCR mixture (20 μl final volume) consisted of 75 ng cDNA, 1 μM of forward and reverse primers, and 1 × Power SYBR Green PCR Master Mix (Applied Biosystems) was used to perform PCR analysis. Amplification and detection were performed using the ABI 7500. The real-time PCR system was designated as the following PCR reaction profile: 95°C for 10 min, and 40 cycles of 95°C for 15 s and 60°C for 1 min, followed by the dissociation curve. All target mRNA data ($n = 4$ for each treatment group) were normalized to villin mRNA for intestinal samples and Gapdh mRNA for liver samples. Levels of villin or Gapdh in the intestine for each segment and liver, respectively were not altered by 1,25$(OH)_2D_3$ treatment. Data were analyzed using the ABI Sequence Detection software version 1.4 to obtain the critical threshold cycle (C_T) value, the cycle number at which the fluorescence increased linearly. For intestinal samples, the C_T value of

Table 1. Rat primer sets for quantitative real-time PCR

	Gene bank number	Forward (5′→3′ sequence)	Reverse (5′→3′ sequence)
Gapdh	XR_007996	CGCTGGTGCTGAGTATGTCG	CTGTGGTCATGAGCCCTTCC
Villin	NM_001108224	GCTCTTTGAGTGCTCCAACC	GGGGTGGGTCTTGAGGTATT
Mrp2	NM_012833	CTGGTGTGGATTCCCTTGG	CAAAACCAGGAGCCATGTGC
Mrp3	NM_080581	ACACCGAGCCAGCCATATAC	TCAGCTTCACATTGCCTGTC
Mrp4	NM_133411	GCCCTTACCCAGCTGCTGA	CAGAATCCAGAGAGCCTCTTTTACA
Oatp1a1	NM_017111	CTACTGCCCTGTTCAAGGCC	ATTGTATCTCTCAGGATTCCGAGG
Oatp1a4	NM_131906	TGCGGAGATGAAGCTCACC	TCCTCCGTCACTTTCGACCTT
Oatp1b2	NM_031650	AGACGTTCCCATCACAACCAC	GCCTCTGCAGCTTTCCTTGA
Asbt	NM_017222	TCAGTTTGGAATCATGCCTCTCA	ACAGGAATAACAAGCGCAACCA
Ostα[a]	NM_001107087	TGTCATCCTGACCGCCCT	AAGCGATCTGCCCGCTG
Ostβ	XM_001076555	TATTCCATCCTGGTTCTGGCAGT	CGTTGTCTTGTGGCTGCTTCTT
Mdr1a	AY582535	GGAGGCTTGCAACCAGCATTC	CTGTTCTGCCGCTGGATTTC
Bsep	XM_579531	TGGAAAGGAATGGTGATGGG	CAGAAGGCCAGTGCATAACAGA
Ntcp	NM_017047	CTCCTCTACATGATTTTCCAGCTTG	CGTCGACGTTCGTTCCTTTTCTTG
Cyp3a1	NM_013105	GGAAATTCGATGTGGAGTGC	AGGTTTGCCTTTCTCTTGCC
Cyp3a2	XM_573414	AGTAGTGACGATTCCAACATAT	TCAGAGGTATCTGTGTTTCCT
Cyp3a9	U60085	GGACGATTCTTGCTTACAGG	ATGCTGGTGGGCTTGCCTTC
Cyp7a1	X17595	CTGTCATACCACAAAGTCTTATGTCA	ATGCTTCTGTGTCCAAATGCC
Cyp24	NM_201635	GCATGGATGAGCTGTGCGA	AATGGTGTCCCAAGCCAGC
VDR	NM_017058	ACAGTCTGAGGCCCAAGCTA	TCCCTGAAGTCAGCGTAGGT
LXRα	NM_031627	TCAGCATCTTCTCTGCAGACCGG	TCATTAGCATCCGTGGGAACA
FXR	NM_021745	AGGCCATGTTCCTTCGTTCA	TTCAGCTCCCCGACACTTTT
SHP	BC088117	CCTTGGCTAGCTGGGTACCA	GTCCCAAGGAGTACGCATACCT
LRH-1	NM_021742	GCTGCCCTGCTGGACTACAC	TGTAGGGCACATCCCCATTC
FGF15	AB078900	ACGGGCTGATTCGCTACTC	TGTAGCCCAAACAGTCCATTTCCT
HNF-1α	X54423	CTCCTCGGTACTGCAAGAAACC	TTGTCACCCCAGCTTAAGACTCT
HNF-4α	EF193392	CCAGCCTACACCACCCTGGAGTT	TTCCTCACGCTCCTCCTGAA

[a]Ostα primer set includes probe 5′ FAM-CAGCCCTCCATTTTCTCCATCTTGGC-TAMRA 3′ for Taqman® gene expression assay.

DOI: 10.1002/bdd

villin was subtracted from the C_T value of the target gene ($\Delta C_T = C_{T.\ target} - C_{T.\ villin}$). The ΔC_T was then compared with the corresponding ΔC_T of the vehicle control ($\Delta\Delta C_T$) and expressed as the fold expression $2^{(\Delta\Delta C_T)}$.

Statistical analysis

The results were expressed as mean ± standard deviation. Data comparing the difference between two groups were analyzed using the two-tailed Student's *t*-test, ANOVA, and Mann-Whitney U-test for errors that were normally distributed or non-normally distributed, respectively. For intestinal and colon mRNA and protein analyses, the vehicle-treated S1 sample (value set as unity for normalization) was used for the normalization of other vehicle- and $1,25(OH)_2D_3$-treated samples in other segments and colon. For liver mRNA and protein analyses, the vehicle-treated sample was usually set as the control (value set as unity), and was used for comparison with those of the treated samples. A value of $p < 0.05$ was set as the level of significance.

Results

Effect of $1,25(OH)_2D_3$ treatment on portal bile acid and alanine aminotransferase (ALT) levels

The total bile acid concentration for the highest $1,25(OH)_2D_3$ dose (2.56 nmol/kg) was significantly higher (55%) compared with that of the control (Table 2). However, there was no change in the levels of ALT in serum, suggesting a lack of damage to the liver by the treatment of $1,25(OH)_2D_3$ at the doses chosen.

Effect of $1,25(OH)_2D_3$ treatment on NRs, enzymes and transporters in intestinal segments and colon

The abundance of mRNA and protein of NRs, transporters, and enzymes in the small intestine was examined under control conditions and compared with those in the colon. The effects of $1,25(OH)_2D_3$ on transporter and enzyme expression were then studied in the segment(s) of greatest abundance.

Nuclear receptors (NRs). Intestinal NRs were found to be distributed differentially in the small intestine and colon. The mRNA distribution of VDR revealed a slight decreasing gradient, from the duodenum to ileum, and the level was significantly higher in the colon (1.23-fold of duodenum) (Figure 1A). VDR protein, however, was relatively evenly distributed in the small intestine and the colon (Figure 1A). The mRNA and protein levels of liver VDR were 1% and 14% those of S1, respectively (Figure 1A). The $1,25(OH)_2D_3$-treated rats exhibited little change in intestinal VDR mRNA and protein (Figure 1B) although VDR protein increased by 50% in the S2 for the 1.28 nmol/kg treated group (Figure 1B).

Unlike VDR, the mRNA distribution of FXR mRNA increased from the duodenum to ileum, and was highest in the colon (Figure 2A). There was no induction of FXR mRNA except for a small increase in the colon for the 1.28 nmol/kg treatment group (Figure 2A). Surprisingly, the distribution of SHP in the small intestine is in sharp contrast to that of FXR (Figure 2B). The expression of SHP mRNA was evenly distributed in the small intestine and was highest in the colon, and this intestinal distribution pattern of SHP was similar to that observed by others for

Table 2. Changes in body weight and blood analysis with various intraperitoneal injections of 1,25-dihydroxyvitamin D_3 treatment for 4 days to the rat *in vivo*

	Daily dose of $1,25(OH)_2D_3$ (nmol/kg/day)				
	0	0.64	1.28	2.56	ANOVA
Portal bile acid (μg/ml)	41.9 ± 7.8	44.6 ± 10.1	49.9 ± 16.8	65.1 ± 14.9[a]	[b]
Alanine aminotransferase, ALT (IU/l)	11.7 ± 8.2	19.9 ± 2.3	12.0 ± 4.5	17.1 ± 7.1	

[a] $p < 0.05$, compared with vehicle treatment (0 nmol $1,25(OH)_2D_3$/kg/day) using two-tailed Student's *t*-test.
[b] $p < 0.05$, ANOVA.

DOI: 10.1002/bdd

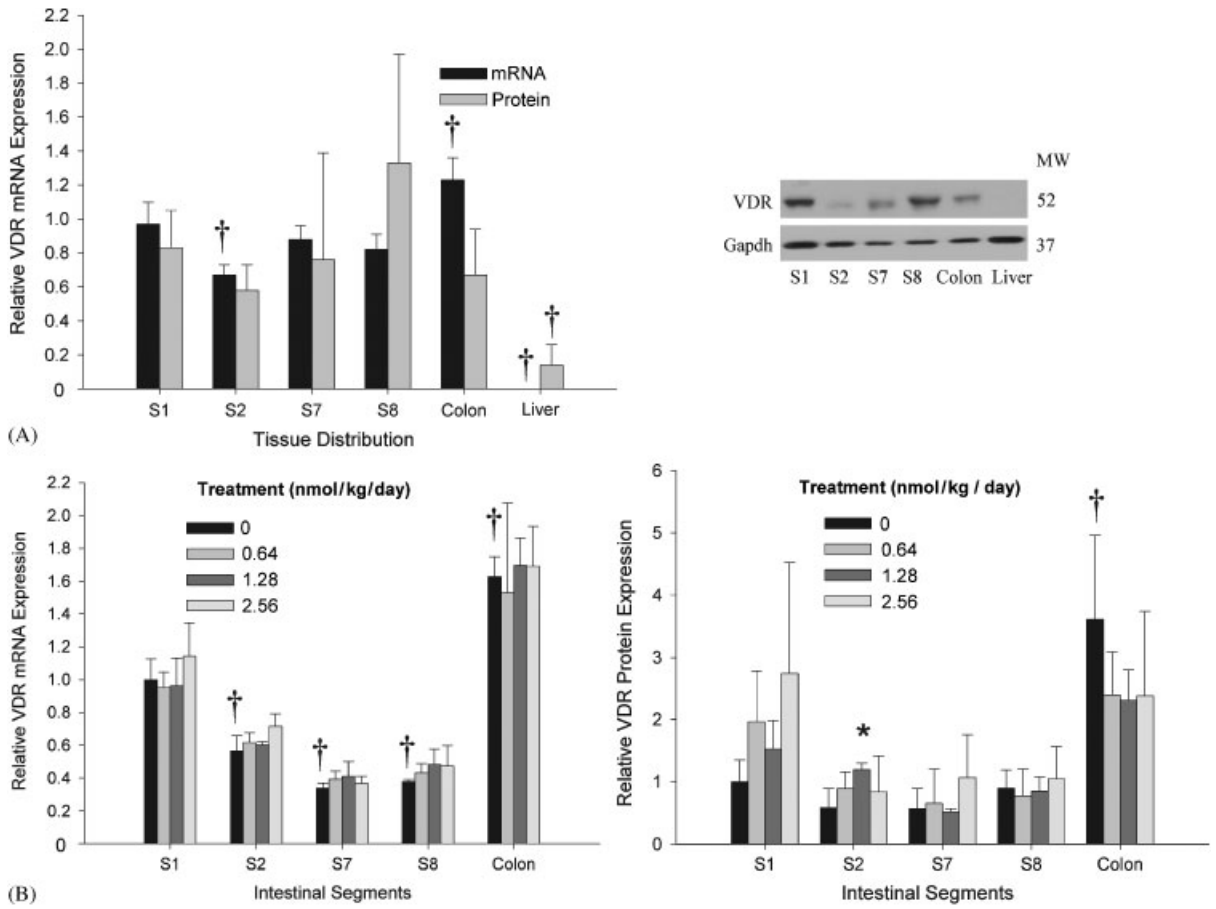

Figure 1. Distribution and dose-dependent effects of $1,25(OH)_2D_3$ on rat intestinal VDR mRNA and protein ($n = 3$ or 4 in each group). (a) mRNA and protein distributions of VDR in the small intestine [duodenum (S1), proximal jejunum (S2), distal jejunum (S7) and ileum (S8)], colon and liver are shown, normalized to Gapdh expression. (b) mRNA and protein changes of VDR, normalized to villin. The molecular weights of Gapdh, VDR and villin bands were detected at 37, 52 and 95 kDa, respectively. $^{*}p < 0.05$ compared with vehicle control in the same segment, $^{\dagger}p < 0.05$ compared with the level of vehicle-control S1 segment using the two-tailed Student's *t*-test

the rat small intestine [32]. A 2- to 6-fold induction in SHP mRNA was observed for the proximal jejunum and ileum relative to the control, as found previously [19]. Similar to FXR, the expression of LRH-1 mRNA increased from the duodenum to ileum, and was highest in the colon (Figure 2C); LRH-1 mRNA was relatively unaltered by $1,25(OH)_2D_3$ treatment in the small intestine, though a small (36%) increase occurred at the highest $1,25(OH)_2D_3$ dose in S1 (Figure 2C). Since the mRNA expression of FGF15 was highest in the ileum in mice [7], our appraisal of the induction in tissue of the S8 segment showed at least a 3-fold increase in the $1,25(OH)_2D_3$ treated tissue over that of the control group (Figure 3).

Enzymes. Intestinal Cyp3a1 and Cyp3a9 mRNAs were preferentially localized in proximal segments of the small intestine, and was lowest in the colon (Figure 4A and B), whereas Cyp3a2 mRNA was virtually undetectable (data not shown). All of the $1,25(OH)_2D_3$ doses resulted in a significant induction (>10-fold of control) of Cyp3a1 mRNA in S1 and S2 segments (Figure 4A), where the expression was most prominent for total Cyp3a protein (all Cyp3a1, Cyp3a2, Cyp3a9 isoforms) [33]. On the other hand, intestinal Cyp3a9 mRNA was

DOI: 10.1002/bdd

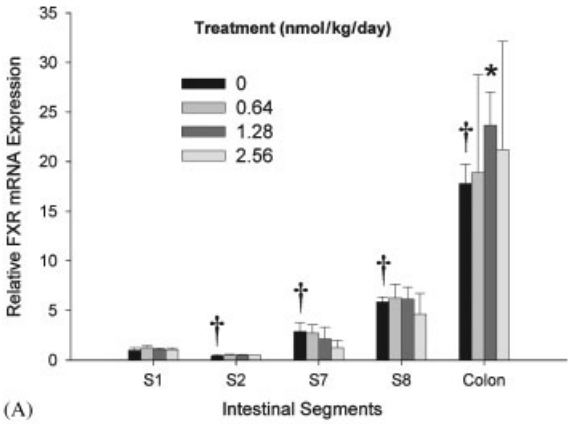

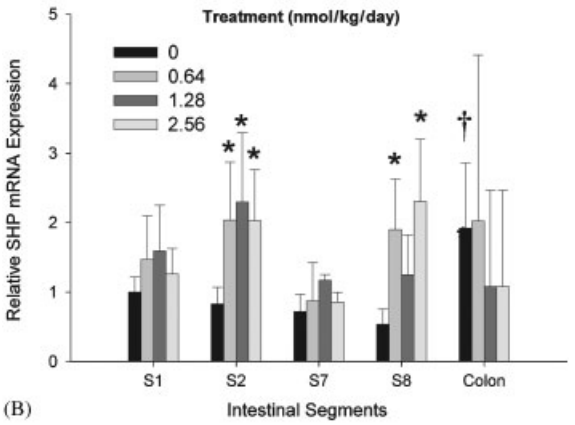

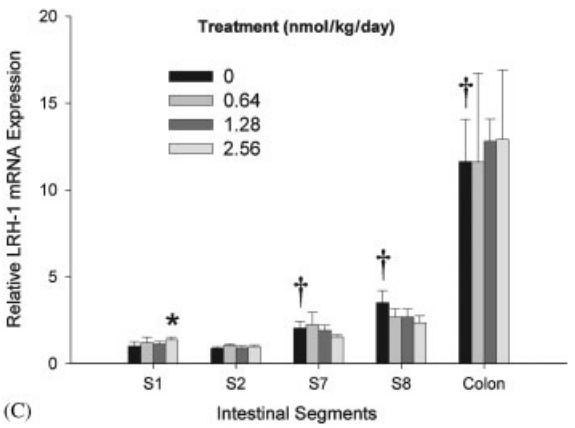

Figure 2. Distribution and dose-dependent effects of $1,25(OH)_2D_3$ on intestinal (a) FXR, (b) SHP and (c) LRH-1 mRNA ($n = 3$ or 4 in each group). $^*p < 0.05$ compared with vehicle control in the same segment, $^\dagger p < 0.05$ compared with the level of vehicle-control S1 segment using the two-tailed Student's *t*-test

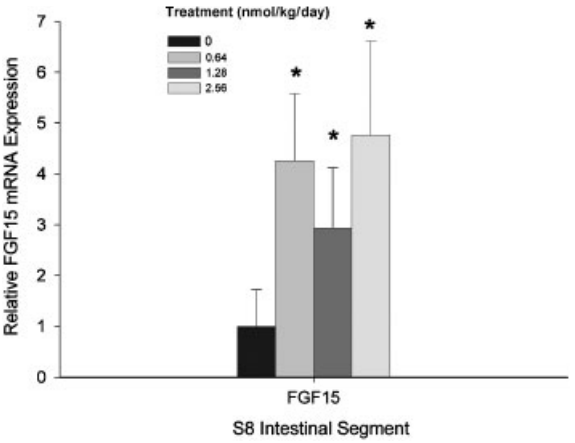

Figure 3. Dose-dependent effects of $1,25(OH)_2D_3$ on intestinal FGF15 mRNA in the ileum ($n = 3$ or 4 in each group). "*" indicates $p < 0.05$ compared to vehicle control in the same segment using the two-tailed Student's *t*-test

unperturbed in rats treated for 4 days with $1,25(OH)_2D_3$ (Figure 4B). Dose-dependent increases of total Cyp3a protein (>2-fold) were clearly observed with $1,25(OH)_2D_3$ treatment (Figure 4C). Cyp24, a catabolic enzyme that inactivates $1,25(OH)_2D_3$ [34,35], was present at low level along the small intestine, and levels of this signature VDR enzyme that responds to $1,25(OH)_2D_3$ [36,37], was significantly induced after $1,25(OH)_2D_3$ treatment (>2-fold, $p < .05$; data not shown).

Apical absorptive transporter. Asbt mRNA was most abundant in the rat ileum (S8) [19], and only 1% mRNA was found in the colon (data not shown). These levels were unchanged with $1,25(OH)_2D_3$ treatment (Figure 5A). Asbt protein, present most abundantly in S8 [19], was increased significantly for the 2.56 nmol/kg treatment group (Figure 5B).

Basolateral efflux transporter. Ostα and Ostβ mRNA, noted to be localized mostly in the ileum [11], was modestly induced by the lowest dose of $1,25(OH)_2D_3$ (Figure 6), but was decreased at the higher doses.

Effect of $1,25(OH)_2D_3$ on hepatic nuclear receptors, enzymes, and transporters

Nuclear receptors (NRs). More significant changes were observed for the mRNA expression of NRs in the liver (Table 3). At the highest

DOI: 10.1002/bdd

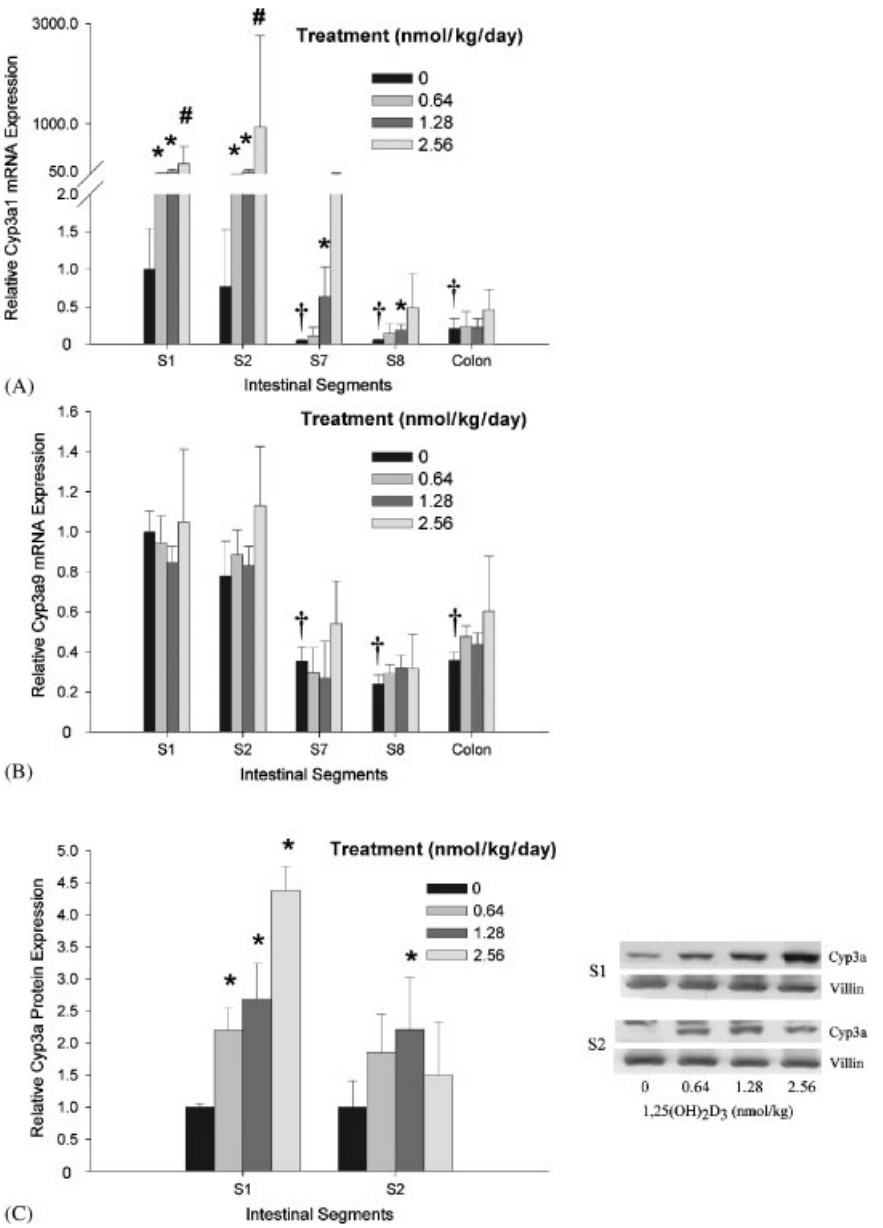

Figure 4. Distribution and dose-dependent effects of $1,25(OH)_2D_3$ on intestinal Cyp3a enzymes ($n = 3$ or 4 in each group). The distribution and changes in Cyp3a1 (A) and Cyp3a9 (B) mRNA and changes in Cyp3a protein in S1 and S2 segments (C) with $1,25(OH)_2D_3$ treatments are shown. The Cyp3a protein band was detected at 56 kDa. Cyp3a protein for S1 and S2 controls were viewed as unity. $^*p < 0.05$ compared with vehicle control in the same segment, $^\dagger p < 0.05$ compared with the level of vehicle-control S1 segment using the two-tailed Student's *t*-test. $^\ddagger p < 0.05$ compared with vehicle control in the same segment using the Mann-Whitney U test

$1,25(OH)_2D_3$ dose (2.56 nmol/kg), FXR and VDR mRNA levels exhibited a 43% to 75% increase over those of controls. SHP mRNA was also significantly induced (2.5- to 5-fold) (Table 3). In addition, significant increases in LRH-1 and LXRα mRNA were observed at doses exceeding 1.28 nmol/kg; HNF-4α and HNF-1α mRNA expressions were increased at the highest dose, though the increase (about 37%) was modest (Table 3).

DOI: 10.1002/bdd

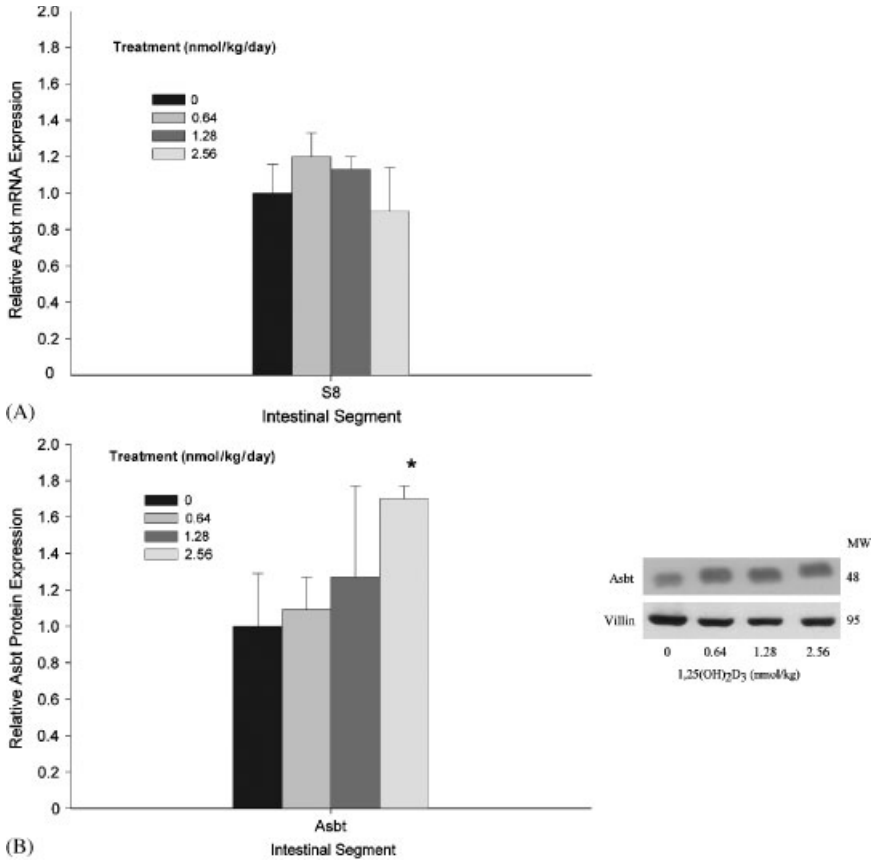

Figure 5. Dose-dependent effects of $1,25(OH)_2D_3$ on intestinal mRNA and protein of Asbt in the ileum ($n = 3$ or 4 in each group). Asbt mRNA (A) and protein (S8) with $1,25(OH)_2D_3$ treatment are shown; the Asbt protein band was detected at 48 kDa in the ileum (S8). $^{*}p < 0.05$ compared with vehicle control in the same segment using the two-tailed Student's *t*-test

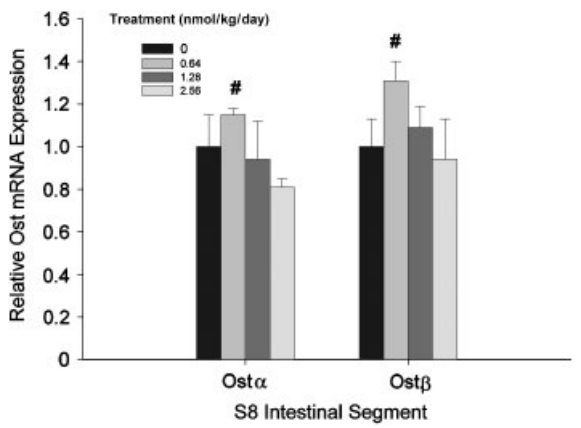

Figure 6. Dose-dependent effects of $1,25(OH)_2D_3$ on intestinal Ostα and Ostβ mRNA in the ileum ($n = 3$ or 4 in each group). $^{\#}p < 0.05$ compared with vehicle control in the same segment using the Mann-Whitney U test

P450s. In the liver, only Cyp3a2 mRNA was significantly induced (66%) over that of the control at the highest dose, whereas Cyp3a1 mRNA remained unchanged; the small increase in mRNA expressions of Cyp3a9 was insignificant (Table 3). A probable explanation is that only Cyp3a2 is present in bile duct epithelial cells [15] where VDR is present [27,38], whereas all Cyp3a1, Cyp3a2 and Cyp3a9 are found in hepatocytes [38] where VDR is very low. In liver, the total Cyp3a protein was unchanged. Levels of Cyp24 mRNA were very low, and were not altered with $1,25(OH)_2D_3$ treatment (data not shown).

The mRNA level of Cyp7a1 was unchanged (Table 3), but there was a significant reduction in Cyp7a1 protein (>50%) at all doses of $1,25(OH)_2D_3$ treatment (Figure 7A). Moreover, Cyp7a1 activity

DOI: 10.1002/bdd

Table 3. Changes in mRNA expression of rat hepatic nuclear receptors, enzymes, and transporters, expressed as fold expression compared with vehicle treatment

		$1,25(OH)_2D_3$ dose (nmol/kg/day)				
	Gene	0	0.64	1.28	2.56	ANOVA
Hepatic nuclear receptors	FXR	1.00±0.13	1.36±0.38	1.17±0.23	1.43±0.28[a]	
	SHP	1.00±0.55	2.66±0.55[a]	2.65±0.64[a]	4.93±3.18[b]	[c]
	LXRα	1.00±0.10	1.23±0.24	1.23±0.11[a]	1.71±0.09[a]	
	HNF-1α	1.00±0.06	0.96±0.13	0.92±0.14	1.37±0.34[b]	
	HNF-4α	1.00±0.12	1.15±0.17	1.15±0.20	1.37±0.22[a]	
	LRH-1	1.00±0.18	1.18±0.23	1.41±0.11[a]	1.63±0.20[a]	
Hepatic cytochrome P450s	Cyp7a1	1.00±0.05	0.96±0.41	1.36±0.98	1.54±0.66	
	Cyp3a1	1.00±0.44	0.74±0.16	0.90±0.54	0.71±0.11	
	Cyp3a9	1.00±0.85	1.00±0.61	2.02±1.62	2.15±1.12	
Hepatic sinusoidal transporters	Ntcp	1.00±0.10	1.09±0.15	1.19±0.26	1.29±0.28	
	Oatp1a1	1.00±0.14	0.96±0.07	0.96±0.14	1.14±0.07	
	Oatp1a4	1.00±0.52	0.68±0.15	0.72±0.28	0.75±0.37	
	Oatp1b2	1.00±0.20	0.90±0.15	0.95±0.13	1.10±0.17	
	Mrp3	1.00±0.22	1.11±0.32	1.18±0.32	2.14±0.81[a]	
	Mrp4	1.00±0.09	0.98±0.21	0.93±0.47	1.27±0.58	
Cholangiocyte	VDR	1.00±0.11	1.34±0.72	1.17±0.29	1.75±0.23[a]	
	Cyp3a2	1.00±0.21	0.95±0.19	1.61±0.65	1.66±0.36[a]	
	Asbt	1.00±0.26	0.78±0.24	0.89±0.38	0.68±0.29	
	Ostα	1.00±0.11	1.53±0.75	1.34±0.33	2.24±0.97[a]	
	Ostβ	1.00±0.34	0.65±0.13	0.56±0.10	0.79±0.33	
Hepatic canalicular transporters	Bsep	1.00±0.07	1.04±0.09	1.17±0.23	1.36±0.21[a]	
	Mrp2	1.00±0.19	1.14±0.21	1.05±0.18	0.94±0.26	
	Mdr1a	1.00±0.27	1.98±0.50[a]	1.78±0.83	2.26±0.84[a]	[c]

[a] $p<0.05$, compared with vehicle treatment (0 nmol $1,25(OH)_2D_3$/kg/day) using the two-tailed Student's *t*-test.
[b] $p<0.05$, compared with vehicle treatment (0 nmol $1,25(OH)_2D_3$/kg/day) using the Mann-Whitney U test.
[c] $p<0.05$, ANOVA.

in rat liver microsomes (4 mg/ml) was reduced significantly from 0.81±0.14 nmol/h/mg in controls to 0.32±0.14 nmol/h/mg protein in $1,25(OH)_2D_3$ (2.56 nmol/kg/day) treated rats ($p = 0.002$; $n = 4$ in each group). The 60% reduction in Cyp7a1 activity observed for the $1,25(OH)_2D_3$-treated rats correlated well with the reduction of protein (Figure 7A) and increased mRNA levels of FXR and SHP.

Transporters. Relatively little change was observed for the sinusoidal and cholangiocytic uptake and efflux transporters in the $1,25(OH)_2D_3$ treated livers. The mRNA and protein expressions for the sinusoidal transporters, Ntcp, Oatp1a1, Oatp1a4, and Oatp1b2, and Ostβ, and the mRNA expression of the cholangiocyte uptake transporter, Asbt [39], were unaltered (Table 3 and Figure 7B). The increase in Mrp3 and Mrp4 protein was not significant in the liver (Figure 7B). Observable changes in the liver were confined to mRNA expressions of Ostα and Mrp3, and the canalicular transporters, Bsep and rat multidrug resistance protein 1a (Mdr1a), especially at the highest dose (Table 3). Moreover, induction of protein was observed for P-gp (Figure 7C, $p<0.05$).

Discussion

This study unequivocally demonstrated that, in addition to FXR, there is a role for $1,25(OH)_2D_3$-liganded VDR on the regulation of transporters and enzymes associated with bile acid homeostasis in the rat. The direct effects of $1,25(OH)_2D_3$ activated VDR in the rat intestine and liver were tissue-specific and related to the presence of VDR. Levels of VDR in the intestine were much higher than those in the liver (Figure 1A). VDR was found to be localized in rat cholangiocytes and stellate cells, and was virtually absent in hepatocytes of the rat [27,38]. Humans, however, have slightly higher VDR levels that are localized both in hepatocytes and cholangiocytes [27,38]. Thus, larger changes due

DOI: 10.1002/bdd

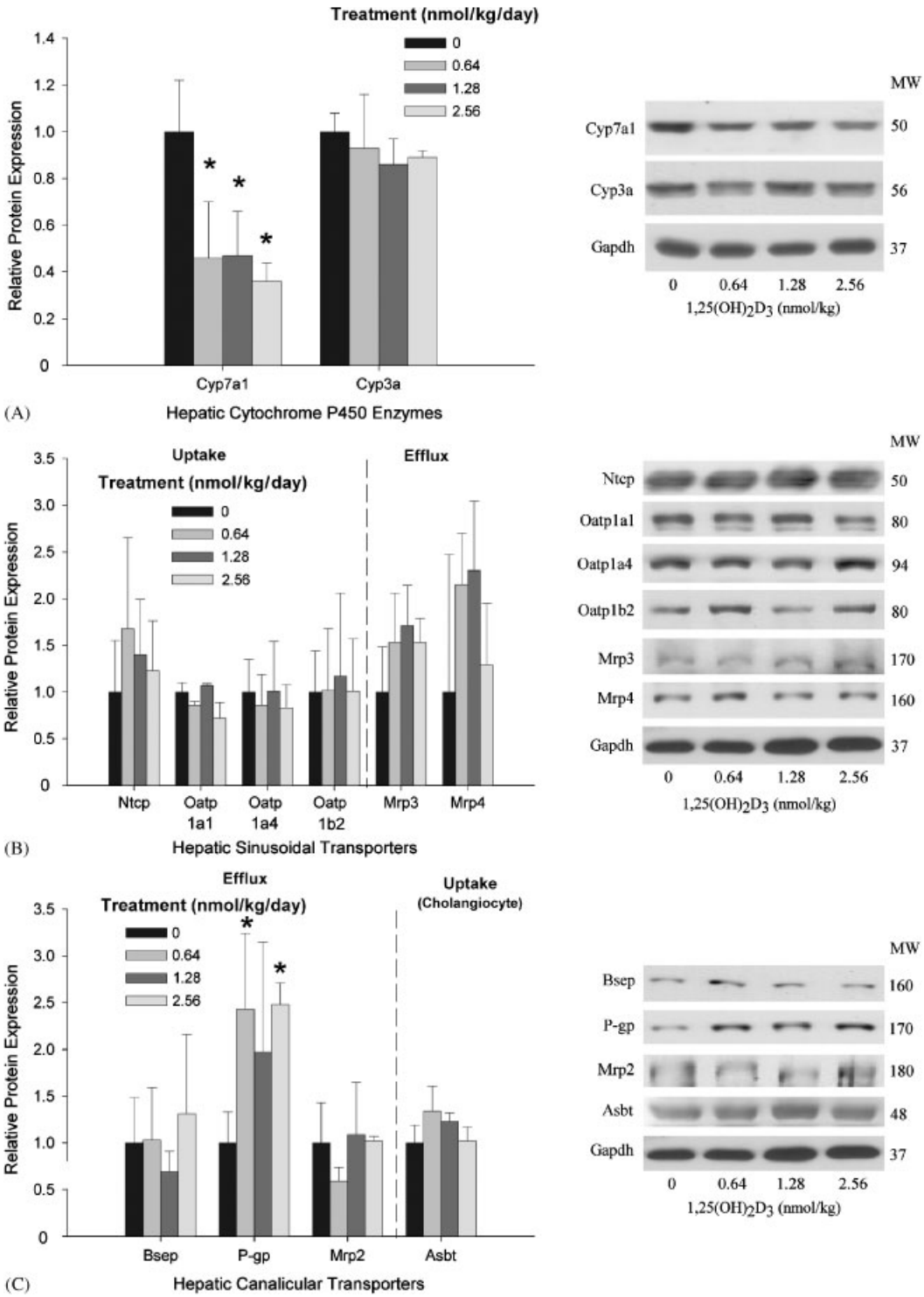

Figure 7. Dose-dependent effects of $1,25(OH)_2D_3$ on changes in protein of hepatic cytochrome P450 isozymes (A), and sinusoidal (B) and canalicular (C) transporters ($n = 3$ or 4 in each group). Gapdh, Cyp7a1, Ntcp, Oatp1a1, Oatp1a4, Oatp1b2 and Bsep bands were detected at 37, 50, 50, 80, 94, 80, and 160 kDa, their molecular weights, respectively. $^*p < 0.05$ compared with vehicle control using the two-tailed Student's *t*-test

DOI: 10.1002/bdd

to VDR were expected for the rat small intestine, whereas lesser or no change was expected for the liver. The administered doses of $1,25(OH)_2D_3$ increased the calcium concentration in plasma without affecting the phosphorous concentration (results not shown). The treatment did not induce liver toxicity (Table 2), but slightly reduced the weight gain of the rats after 4 days of treatment (results not shown). Following the subcutaneous injection of radiolabeled $1,25(OH)_2D_3$, the liver was reported to receive only one third or one quarter of the $1,25(OH)_2D_3$ exposure compared with the duodenum [40]. In addition, the expression of VDR in the intestine compared with the liver is a few thousand fold higher [41]. Although Gascon-Barre *et al*. [27] showed that VDR level in the biliary cells was only 3 times lower than the VDR in the intestine, these biliary cells represented only 5% of the cells in a normal liver [42], and hence VDR abundance is low. Hence, the role of VDR in the liver may be insignificant compared with the intestine in view of the lower expression of VDR and the lower exposure to $1,25(OH)_2D_3$.

A correlation between VDR levels and $1,25(OH)_2D_3$-mediated induction of Cyp3a was clearly observed in the rat small intestine (Figures 1 and 4). Up-regulation of intestinal Cyp3a1 and not Cyp3a9 mRNA was noted, as also observed in rat intestinal slices [15]. These results contrasted with reports on increased Cyp3a9 mRNA in rats that were treated with $1,25(OH)_2D_3$ *in vivo* [16]. Total Cyp3a protein induction, likely Cyp3a1 due to the induction of Cyp3a1 mRNA, and high levels of VDR were observed (Figure 4A–C). Induction of Cyp3a1 but not of Cyp3a9 mRNA was also observed for rat intestinal slices incubated with 100 nM of $1,25(OH)_2D_3$ [15]; Cyp3a2 mRNA was also found and induced in the ileum. In the liver, induction of each of the Cyp3a isozymes was VDR- and site-specific. Induction of mRNA expression of only Cyp3a2 was observed (Table 3), reportedly present in biliary epithelial cells, sites which are co-incident with the localization of VDR [27,38]. However, the hepatic Cyp3a1 and Cyp3a9 mRNA remained unchanged, as observed also in rat liver slice experiments [15]. The absence of change was explained by the absence of VDR in hepatocytes. There may be at least two explanations why Cyp3a proteins are not induced in the liver, but are increased in the intestine. First, Brown *et al*. [40] had shown that the liver received a lower $1,25(OH)_2D_3$ exposure than the intestine when radiolabeled $1,25(OH)_2D_3$ was given subcutaneously to the rat. The study was unable to measure the intracellular $1,25(OH)_2D_3$ concentration in the liver and intestine because of the lack of a sensitive assay and because the half-life of $1,25(OH)_2D_3$ is very short [43,44]. Second, VDR levels are very low in the rat liver and absent in hepatocytes [27,38]. These facts can explain why Cyp3a protein was not increased in the liver by VDR. However, a change was observed for Cyp3a2 mRNA that is colocalized with the VDR in cholangiocytes (Table 3). Upon comparison between the intestine and liver, Cyp3a1 of the small intestine and Cyp3a2 in the liver were induced by the VDR, and Cyp3a9 was not modulated in these organs.

Additional changes observed for transporters and enzymes of the intestine and liver with $1,25(OH)_2D_3$ treatment in the rat *in vivo* are summarized in Figure 8. In the intestine, induction of Asbt (Figure 5B) by $1,25(OH)_2D_3$-liganded VDR [19] led to an increase in portal bile acid concentration (Table 2). Due to the lack of negative feedback mechanism of FXR-SHP-LRH-1 on Asbt because of absence of the LRH-1 *cis* acting element in the rat Asbt promoter [12], Asbt protein increased in response to $1,25(OH)_2D_3$ (Figure 5B). This, together with increased Ostα-Ostβ, triggered increased bile acid absorption in enterocytes, leading to increased bile acid efflux into the portal blood (Table 2). In addition, increased bile acids into enterocytes activated FXR targeted genes. Inagaki *et al*. [7] had shown FXR activation in mice after GW4064 treatment (FXR ligand) with increased mRNA expression of the targets, SHP and FGF15, *in vivo* and decreased Cyp7a1 expression in the mouse liver without changes in FXR. Similarly, our study showed that that mRNA levels of the target genes, SHP, Ostα, Ostβ and FGF15, were increased in the ileum as indicators of the activation by FXR.

Sequentially, the increased bile acid present in the portal vein could elicit FXR-related changes. Changes in the liver, other than Cyp3a2, were observed, and were mostly FXR-related events.

DOI: 10.1002/bdd

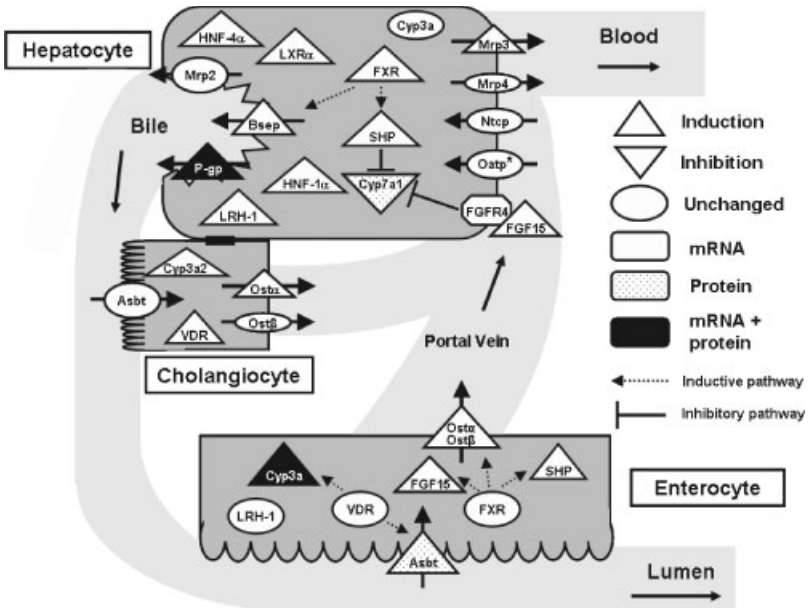

Figure 8. A schematic diagram highlighting direct and indirect effects of $1,25(OH)_2D_3$ on intestinal and hepatic nuclear receptors, drug transporters and enzymes. Cyp3a and Asbt protein were up-regulated by VDR. As a result, the absorption of bile acids into enterocytes was increased, which in turn, activated the intestinal FXR and increased SHP, FGF15, Ostα and Ostβ. Intestinal FGF15 became bound to FGFR4 in liver to inhibit liver Cyp7a1. In liver, FXR and SHP were activated by bile acids and resulted in up-regulation of Bsep, Mrp3 and Ostα mRNA, and down-regulation of hepatic Cyp7a1 protein. *represents the Oatp isoforms, Oatp1a1, Oatp1a4 and Oatp1b2

Elevated FXR-SHP (Table 3) and FGF15 (Figure 3) would down-regulate Cyp7a1 in the liver [2,6,7]. Indeed, there was decreased Cyp7a1 protein (Figure 7A) and lessened microsomal Cyp7a1 activity (60%); the lack of correlation with Cyp7a1 mRNA was, however, unexplained. Other factors might be involved in stabilizing the mRNA expression, and more studies are needed to clarify this mechanism. That the effects of $1,25(OH)_2D_3$ on Cyp7a1 in the liver *in vivo* were caused by indirect FXR effects was confirmed direct incubation of rat liver slices *in vitro* with $1,25(OH)_2D_3$ which failed to alter Cyp7a1, whereas similar incubations with chenodeoxycholic acid decreased Cyp7a1 [38]. In other reports, a reduction (73%) in Cyp7a1 activity in rats has been attributed to the bile acid, deoxycholic acid [31]. In addition, Inagaki *et al*. [7] reported that FGF15 could down-regulate Cyp7a1 in the liver through a mechanism involving FGFR4 and the *c-Jun N*-terminal kinase (JNK)-dependent pathway [45]. In this study, we believe that the synergy of increased FXR and SHP in the liver (Table 3) due to elevated bile acids (Table 2) and the increase in FGF15 (Figure 3) in the intestine resulted in the decrease in Cyp7a1 protein (Figure 7A) and reduction in Cyp7A1 activity.

Pro-inflammatory cytokines such as IL-6 and TNFα, produced by monocytes/macrophages, were found to affect the expression of hepatic transporters and enzymes [46], and these inflammatory factors are known to be regulated by $1,25(OH)_2D_3$ *in vitro* [47,48]. However, similar results were not known *in vivo*. Thus far, the FGF15 (ortholog of human FGF19) is the other endogenous molecule, beside bile acids, that regulates Cyp7a1 *in vivo* [7]. This endogenous signaling molecule is produced mostly in the mouse ileum and is absent in the liver and colon. Although Song *et al*. [6] had reported an increase in FGF19 mRNA in the liver with bile acid treatment, we failed to detect FGF15 mRNA in the rat liver (data not shown). Thus, it is concluded that the increase in ileal FGF15 mRNA is the species responsible for the activation of the signaling pathway that lead to the down-regulation of Cyp7a1 in the rat liver.

DOI: 10.1002/bdd

Furthermore, higher mRNA levels of Bsep and Ostα, other FXR-target genes, were also observed (Table 3). Other effects of $1,25(OH)_2D_3$ on liver transporters were confined to Mrp3 and Mdr1a mRNA and P-gp protein (Table 3 and Figure 7C). Zollner *et al*. [49] have reported that hepatic Mrp3 levels in *fxr*(+/+) and *fxr*(−/−) mice were elevated with cholic acid and ursodeoxycholic acid treatment, suggesting a FXR-independent mechanism for Mrp3 induction. Martin *et al*. [50] showed that chenodeoxycholic acid treatment induced MDR1 mRNA and protein expressions in HepG2. Unfortunately, there was no change for other FXR-related and HNF-4α-related transporters of the liver: Ntcp, Asbt, Oatp1a1, Oatp1a4 and Oatp1b2 (Figure 7B and C). The study also failed to show, in control- and $1,25(OH)_2D_3$-treated groups (0.64 nmol/kg/day × 4), a change in the steady state hepatic extraction ratio of [^{3}H]cholylsarcosine, a substrate of Ntcp and Bsep [19], (0.89 ± 0.1 vs 0.92 ± 0.002, $p > 0.05$, $n = 3$) or for the glutathione conjugate of bromosulfophthalein, a substrate of Oatp1a1 and Mrp2 [51] (extraction ratios of $= 0.39 \pm 0.1$ vs 0.32 ± 0.07, $p > 0.05$, $n > 4$) (unpublished work of S. Liu, L. Taheri, and K. S. Pang). The lack of change may be the result of the low dose of $1,25(OH)_2D_3$ used for treatment. The VDR effects on other NRs/transcription factor, HNF-1α, HNF-4α, and LRH-1, in the liver were minimal (Table 3). In the absence of a change in LXRα, the stimulatory effect of LXRα (Table 3) on Cyp7a1 [5] appeared to be absent. The antagonism reported for VDR on FXR in the human liver [28] was not evident in the present study in the rat since VDR is absent in hepatocytes.

Due to the low levels of VDR in the rat liver [27,38], we did not expect to observe VDR-mediated effects. However, FXR is present in much greater abundance [1]. The increase in Asbt in the rat ileum with $1,25(OH)_2D_3$ treatment, which in turn can cause an increase in bile acid absorption and activate FXR as well as decrease CYP7A1 in the liver, would not occur in man because of the negative feedback mechanism exerted by FXR on ASBT of the human ileum. The feedback mechanism maintains ASBT levels unchanged and prevents the increased absorption of bile acids [12]. However, parallel increases in Cyp3a/CYP3A enzymes are expected in both the rat and human with $1,25(OH)_2D_3$ treatment [15]. Cyp3a1 mRNA and Cyp3a protein were found increased in a dose-dependent fashion by $1,25(OH)_2D_3$ in the rat S1 and S2 intestinal segments with $1,25(OH)_2D_3$ treatment (Figure 4), and it was also shown that $1,25(OH)_2D_3$ treatment could increase CYP3A4 expression in human intestinal slices *in vitro* [15] and in Caco-2 cells [23].

In summary, it was shown that $1,25(OH)_2D_3$ is capable of altering intestinal and hepatic transporters and enzymes in the rat *in vivo* (Figure 8). Tissue- and enzyme-specific induction by VDR occurred due to the differential abundance of VDR and the dose of $1,25(OH)_2D_3$ administered. Direct VDR changes were found in the rat intestine where higher levels of VDR existed. Rat intestinal Cyp3a1 but not Cyp3a9 mRNA was induced, whereas only Cyp3a2 and not Cyp3a1 or Cyp3a9 mRNA was induced in the rat liver. FXR, SHP, Ostα Bsep and Mrp3 mRNA levels were increased in the rat liver, suggesting that these secondary FXR effects are elicited as a result of increased bile acid absorption by rat Asbt. Repression of hepatic Cyp7a1 protein and activity was observed, likely the result of secondary FXR effects in the liver as well as increased FGF15 in the intestine of the rat. The secondary, FXR-related changes on Cyp7a1 and Bsep in the liver were absent in studies carried out *in vitro* when $1,25(OH)_2D_3$ was incubated directly with liver tissue [37], confirming that these effects were not directly mediated by VDR. Changes in hepatic Mrp3 and Mdr1a mRNA and P-gp protein by $1,25(OH)_2D_3$ were, however, unexplained, but may be FXR-related.

The composite results (Figure 8) emphasize that VDR is an important NR that plays a direct role on intestinal transporters and enzymes, and an indirect role in the induction of FXR-related genes in the liver. Dose-dependent, direct VDR effects of Cyp3a and Asbt in the intestine were observed in this study. In turn, increased bile acid in portal blood activated the FXR in the liver. The results showed that when the mRNA changes of the target genes were highly induced, changes in protein followed. However, small changes in mRNA expression were not always followed by changes in protein expression. Moreover, in a multiple organ system, indirect dose-dependent

DOI: 10.1002/bdd

effects may not be demonstrated clearly since many other factors maybe involved. However, the combination of *in vivo* and *in vitro* experimentation with intestinal and liver slices provided the needed resolution. A dose-dependent effect on the down-regulation of Cyp7a1 protein was observed, which could be the result of the activation of FXR in the liver and of increased FGF-15 production in the ileum. It was confirmed that these are FXR-related effects since the change in Cyp7a1 expression in rat liver slices occurred with bile acids and not $1,25(OH)_2D_3$ incubation *in vitro* [38].

These changes found in the intestine and liver elicited by $1,25(OH)_2D_3$ could potentially affect drug absorption, oral bioavailability and clearances. The consequences of the activation of VDR by $1,25(OH)_2D_3$ or vitamin D analogs on first-pass elimination are paramount, especially with the administration of the vitamin D analogs, an emergent class of therapeutics for the treatment of cancer and other diseases [52,53].

Acknowledgments

We thank Dr Jianghong Fan of our laboratory for assistance in tissue collection and Dr Carolyn Cummins of the University of Toronto for invaluable discussions. Dr Han-Joo Maeng was supported by the Government of Canada Postdoctoral Research Fellowship (PDRF). This work was supported by the Canadian Institutes for Health Research, MOP89850. Edwin Chow was the recipient of the UofT Open Fellowship.

References

1. Zollner G, Marschall HU, Wagner M, Trauner M. Role of nuclear receptors in the adaptive response to bile acids and cholestasis: pathogenetic and therapeutic considerations. *Mol Pharm* 2006; **3**: 231–251.
2. Goodwin B, Jones SA, Price RR, *et al*. A regulatory cascade of the nuclear receptors FXR, SHP-1, and LRH-1 represses bile acid biosynthesis. *Mol Cell* 2000; **6**: 517–526.
3. Chiang JY. Regulation of bile acid synthesis. *Front Biosci* 1998; **3**: d176–d193.
4. Crestani M, Sadeghpour A, Stroup D, Galli G, Chiang JY. Transcriptional activation of the cholesterol 7α-hydroxylase gene (CYP7A) by nuclear hormone receptors. *J Lipid Res* 1998; **39**: 2192–2200.
5. Chiang JY, Kimmel R, Stroup D. Regulation of cholesterol 7α-hydroxylase gene (CYP7A1) transcription by the liver orphan receptor (LXRα). *Gene* 2001; **262**: 257–265.
6. Song KH, Li T, Owsley E, Strom S, Chiang JY. Bile acids activate fibroblast growth factor 19 signaling in human hepatocytes to inhibit cholesterol 7α-hydroxylase gene expression. *Hepatology* 2009; **49**: 297–305.
7. Inagaki T, Choi M, Moschetta A, *et al*. Fibroblast growth factor 15 functions as an enterohepatic signal to regulate bile acid homeostasis. *Cell Metab* 2005; **2**: 217–225.
8. Denson LA, Sturm E, Echevarria W, *et al*. The orphan nuclear receptor, shp, mediates bile acid-induced inhibition of the rat bile acid transporter, ntcp. *Gastroenterology* 2001; **121**: 140–147.
9. Kast HR, Goodwin B, Tarr PT, *et al*. Regulation of multidrug resistance-associated protein 2 (ABCC2) by the nuclear receptors pregnane X receptor, farnesoid X-activated receptor, and constitutive androstane receptor. *J Biol Chem* 2002; **277**: 2908–2915.
10. Trauner M, Boyer JL. Bile salt transporters: molecular characterization, function, and regulation. *Physiol Rev* 2003; **83**: 633–671.
11. Rao A, Haywood J, Craddock AL, Belinsky MG, Kruh GD, Dawson PA. The organic solute transporter α-β, Ostα-Ostβ, is essential for intestinal bile acid transport and homeostasis. *Proc Natl Acad Sci USA* 2008; **105**: 3891–3896.
12. Chen F, Ma L, Dawson PA, *et al*. Liver receptor homologue-1 mediates species- and cell line-specific bile acid-dependent negative feedback regulation of the apical sodium-dependent bile acid transporter. *J Biol Chem* 2003; **278**: 19909–19916.
13. Reschly EJ, Krasowski MD. Evolution and function of the NR1I nuclear hormone receptor subfamily (VDR, PXR, and CAR) with respect to metabolism of xenobiotics and endogenous compounds. *Curr Drug Metab* 2006; **7**: 349–365.
14. Thummel KE, Brimer C, Yasuda K, *et al*. Transcriptional control of intestinal cytochrome P-4503A by 1α,25-dihydroxy vitamin D_3. *Mol Pharmacol* 2001; **60**: 1399–1406.
15. Khan AA, Chow EC, van Loenen-Weemaes AM, Porte RJ, Pang KS, Groothuis GM. Comparison of effects of VDR versus PXR, FXR and GR ligands on the regulation of CYP3A isozymes in rat and human intestine and liver. *Eur J Pharm Sci* 2009; **37**: 115–125.
16. Zierold C, Mings JA, Deluca HF. 19nor-1,25-dihydroxyvitamin D_2 specifically induces CYP3A9 in rat intestine more strongly than

DOI: 10.1002/bdd

1,25-dihydroxyvitamin D_3 *in vivo* and in vitro. *Mol Pharmacol* 2006; **69**: 1740–1747.
17. Xu Y, Iwanaga K, Zhou C, Cheesman MJ, Farin F, Thummel KE. Selective induction of intestinal CYP3A23 by 1α,25-dihydroxyvitamin D_3 in rats. *Biochem Pharmacol* 2006; **72**: 385–392.
18. Makishima M, Lu TT, Xie W, *et al*. Vitamin D receptor as an intestinal bile acid sensor. *Science* 2002; **296**: 1313–1316.
19. Chen X, Chen F, Liu S, *et al*. Transactivation of rat apical sodium-dependent bile acid transporter and increased bile acid transport by 1α,25-dihydroxyvitamin D_3 via the vitamin D receptor. *Mol Pharmacol* 2006; **69**: 1913–1923.
20. Chow ECY, Liu S, Khan AA, Groothuis GMM, Pang KS. Effects of 1α,25-dihydroxyvitamin D_3, the natural ligand of the vitamin D receptor (VDR), on transporters, enzymes, and nuclear receptors in the rat intestine and liver. *AAPS Annual Meeting, Atlanta, GA*, 2008; *AAPS J* 2008; 10(S2) Abstract #1138.
21. McCarthy TC, Li X, Sinal CJ. Vitamin D receptor-dependent regulation of colon multidrug resistance-associated protein 3 gene expression by bile acids. *J Biol Chem* 2005; **280**: 23232–23242.
22. Echchgadda I, Song CS, Roy AK, Chatterjee B. Dehydroepiandrosterone sulfotransferase is a target for transcriptional induction by the vitamin D receptor. *Mol Pharmacol* 2004; **65**: 720–729.
23. Fan J, Liu S, Du Y, Morrison J, Shipman R, Pang KS. Upregulation of transporters and enzymes by the vitamin D receptor (VDR) and ligands [1α,25-dihydroxyvitamin D_3 and vitamin D analogues in the Caco-2 cell monolayer. *J Pharmacol Exp Ther* 2009; **330**: 389–402.
24. Saeki M, Kurose K, Tohkin M, Hasegawa R. Identification of the functional vitamin D response elements in the human MDR1 gene. *Biochem Pharmacol* 2008; **76**: 531–542.
25. Ogura M, Nishida S, Ishizawa M, *et al*. Vitamin D_3 modulates the expression of bile acid regulatory genes and represses inflammation in bile duct-ligated mice. *J Pharmacol Exp Ther* 2009; **328**: 564–570.
26. Theodoropoulos C, Demers C, Petit JL, Gascon-Barre M. High sensitivity of rat hepatic vitamin D_3-25 hydroxylase CYP27A to 1,25-dihydroxyvitamin D_3 administration. *Am J Physiol Endocrinol Metab* 2003; **284**: E138–E147.
27. Gascon-Barre M, Demers C, Mirshahi A, Neron S, Zalzal S, Nanci A. The normal liver harbors the vitamin D nuclear receptor in nonparenchymal and biliary epithelial cells. *Hepatology* 2003; **37**: 1034–1042.
28. Honjo Y, Sasaki S, Kobayashi Y, Misawa H, Nakamura H. 1,25-dihydroxyvitamin D_3 and its receptor inhibit the chenodeoxycholic acid-dependent transactivation by farnesoid X receptor. *J Endocrinol* 2006; **188**: 635–643.
29. Johnson BM, Zhang P, Schuetz JD, Brouwer KL. Characterization of transport protein expression in multidrug resistance-associated protein (Mrp) 2-deficient rats. *Drug Metab Dispos* 2006; **34**: 556–562.
30. Lowry OH, Rosebrough NJ, Farr AL, Randall RJ. Protein measurement with the Folin phenol reagent. *J Biol Chem* 1951; **193**: 265–275.
31. Hylemon PB, Studer EJ, Pandak WM, Heuman DM, Vlahcevic ZR, Chiang JY. Simultaneous measurement of cholesterol 7α-hydroxylase activity by reverse-phase high-performance liquid chromatography using both endogenous and exogenous [4-^{14}C]cholesterol as substrate. *Anal Biochem* 1989; **182**: 212–216.
32. Los EL, Wolters H, Stellaard F, Kuipers F, Verkade HJ, Rings EH. Intestinal capacity to digest and absorb carbohydrates is maintained in a rat model of cholestasis. *Am J Physiol Gastrointest Liver Physiol* 2007; **293**: G615–G622.
33. Liu S, Tam D, Chen X, Pang KS. P-glycoprotein and an unstirred water layer barring digoxin absorption in the vascularly perfused rat small intestine preparation: induction studies with pregnenolone-16α-carbonitrile. *Drug Metab Dispos* 2006; **34**: 1468–1479.
34. Healy KD, Zella JB, Prahl JM, DeLuca HF. Regulation of the murine renal vitamin D receptor by 1,25-dihydroxyvitamin D_3 and calcium. *Proc Natl Acad Sci USA* 2003; **100**: 9733–9737.
35. Meyer MB, Zella LA, Nerenz RD, Pike JW. Characterizing early events associated with the activation of target genes by 1,25-dihydroxyvitamin D_3 in mouse kidney and intestine *in vivo*. *J Biol Chem* 2007; **282**: 22344–22352.
36. Beckman MJ, DeLuca HF. Regulation of renal vitamin D receptor is an important determinant of 1α,25-dihydroxyvitamin D_3 levels *in vivo*. *Arch Biochem Biophys* 2002; **401**: 44–52.
37. Chen KS, DeLuca HF. Cloning of the human 1α,25-dihydroxyvitamin D_3 24-hydroxylase gene promoter and identification of two vitamin D-responsive elements. *Biochim Biophys Acta* 1995; **1263**: 1–9.
38. Khan AA, Chow EC, Porte RJ, Pang KS, Groothuis GM. 1α,25-Dihydroxyvitamin D_3 mediates down-regulation of HNF4α, CYP7A1 and NTCP in human but not in rat liver. 2009: Submitted.
39. Lazaridis KN, Pham L, Tietz P, *et al*. Rat cholangiocytes absorb bile acids at their apical domain via the ileal sodium-dependent bile acid transporter. *J Clin Invest* 1997; **100**: 2714–2721.
40. Brown AJ, Ritter CS, Holliday LS, Knutson JC, Strugnell SA. Tissue distribution and activity studies of 1,24-dihydroxyvitamin D_2, a metabolite of vitamin D_2 with low calcemic activity *in vivo*. *Biochem Pharmacol* 2004; **68**: 1289–1296.
41. Sandgren ME, Bronnegard M, DeLuca HF. Tissue distribution of the 1,25-dihydroxyvitamin D_3

receptor in the male rat. *Biochem Biophys Res Commun* 1991; **181**: 611–616.
42. Racanelli V, Rehermann B. The liver as an immunological organ. *Hepatology* 2006; **43**: S54–S62.
43. Vieth R, Kooh SW, Balfe JW, Rawlins M, Tinmouth WW. Tracer kinetics and actions of oral and intraperitoneal 1,25-dihydroxyvitamin D_3 administration in rats. *Kidney Int* 1990; **38**: 857–861.
44. Kissmeyer AM, Binderup L. Calcipotriol (MC 903): pharmacokinetics in rats and biological activities of metabolites. A comparative study with $1,25(OH)_2D_3$. *Biochem Pharmacol* 1991; **41**: 1601–1606.
45. Holt JA, Luo G, Billin AN, *et al*. Definition of a novel growth factor-dependent signal cascade for the suppression of bile acid biosynthesis. *Genes Dev* 2003; **17**: 1581–1591.
46. Morgan ET, Goralski KB, Piquette-Miller M, *et al*. Regulation of drug-metabolizing enzymes and transporters in infection, inflammation, and cancer. *Drug Metab Dispos* 2008; **36**: 205–216.
47. Kozawa O, Tokuda H, Kaida T, Matsuno H, Uematsu T. Effect of vitamin D_3 on interleukin-6 synthesis induced by prostaglandins in osteoblasts. *Prostaglandins Leukot Essent Fatty Acids* 1998; **58**: 119–123.
48. Golovko O, Nazarova N, Tuohimaa P. Vitamin D-induced up-regulation of tumour necrosis factor alpha (TNF-alpha) in prostate cancer cells. *Life Sci* 2005; **77**: 562–577.
49. Zollner G, Fickert P, Fuchsbichler A, *et al*. Role of nuclear bile acid receptor, FXR, in adaptive ABC transporter regulation by cholic and ursodeoxycholic acid in mouse liver, kidney and intestine. *J Hepatol* 2003; **39**: 480–488.
50. Martin P, Riley R, Back DJ, Owen A. Comparison of the induction profile for drug disposition proteins by typical nuclear receptor activators in human hepatic and intestinal cells. *Br J Pharmacol* 2008; **153**: 805–819.
51. Geng W, Schwab AJ, Horie T, Goresky CA, Pang KS. Hepatic uptake of bromosulfophthalein-glutathione in perfused Eisai hyperbilirubinemic mutant rat liver: a multiple-indicator dilution study. *J Pharmacol Exp Ther* 1998; **284**: 480–492.
52. Trump DL, Hershberger PA, Bernardi RJ, *et al*. Anti-tumor activity of calcitriol: pre-clinical and clinical studies. *J Steroid Biochem Mol Biol* 2004; **89–90**: 519–526.
53. Brown AJ, Slatopolsky E. Vitamin D analogs: therapeutic applications and mechanisms for selectivity. *Mol Aspects Med* 2008; **29**: 433–452.

DOI: 10.1002/bdd